Resting-state functional MR imaging identifies cerebrovascular reactivity impairment in patients with arterial occlusive diseases: A pilot study.

Abstract

BACKGROUND: The development of non-invasive approaches for identifying hypoperfused brain tissue at risk is of major interest. Recently, the temporal-shift (TS) maps estimated from resting-state blood oxygenation level-dependent (BOLD) signals have been proposed for determining hemodynamic state.

OBJECTIVE: To examine the equivalency of the TS map and the cerebrovascular reactivity (CVR) map derived from acetazolamide-challenged single-photon emission computed tomography (SPECT) in identifying hemodynamic impairment in patients with arterial occlusive diseases.

METHODS: Twenty-three patients with arterial occlusive diseases who underwent SPECT were studied. With a recursive TS analysis of low-frequency fluctuation of the BOLD signal, a TS map relative to the global signal was created for each patient. The voxel-by-voxel correlation coefficient was calculated to examine the image similarity between TS and SPECT-based cerebral blood flow (CBF) or CVR maps in each patient. Furthermore, simple linear regression analyses were performed to examine the quantitative relationship between the TS of BOLD signals and CVR in each cerebrovascular territory.

RESULTS: The within-patient, voxel-by-voxel comparison revealed that the TS map was more closely correlated with SPECT-CVR map ([Z(r)] = 0.42 ± 0.18) than SPECT-CBF map ([Z(r)] =

0.058 ± 0.11) ($P < .001$, paired t test). The regression analysis showed a significant linear association between the TS of BOLD signals and CVR in the anterior circulation where the reduction of CVR was evident in the patient group.

CONCLUSION: BOLD TS analysis has potential as a non-invasive alternative to current methods based on CVR for identification of tissue at risk of ischemic stroke.

Key Words: arterial occlusive diseases, cerebrovascular reactivity, functional magnetic resonance imaging, single-photon emission computed tomography

Running Title: BOLD detects abnormal cerebrovascular reactivity

Abbreviations

ACA, anterior cerebral artery; ACZ, acetazolamide; BOLD, blood oxygenation level dependent; CBF. cerebral blood flow; CO_2, carbon dioxide; CVR, cerebrovascular reactivity; FWHM, full width at half maximum; IMP, iodine-123 N-isopropyl-p-iodoamphetamine; MCA, middle cerebral artery; MRI, magnetic resonance imaging; MTT, mean transit time; ROI, region of interest; rs-fMRI, resting-state functional MRI; PCA, posterior cerebral artery; SPECT, single photon emission computed tomography; TS, temporal-shift; TTP, time to peak

Introduction

Assessment of hemodynamic impairment is essential for ischemic stroke risk prediction in patients with arterial occlusive diseases. Hemodynamic status in patients with chronic ischemia is evaluated through measurement of the vasodilatory reserve, which reflects compensatory responses to reduced cerebral perfusion pressure.[1,2] The capacity for compensatory vasodilation is measured as cerebrovascular reactivity (CVR) using various techniques including nuclear medicine modalities, such as positron-emission tomography (PET) and single-photon emission computed tomography (SPECT),[3,4] and magnetic resonance imaging (MRI) [5], with PET and SPECT still being considered the reference method. These tomographic imaging strategies are useful in determining which patients with carotid stenosis [3] or moyamoya disease (MMD) would likely benefit from treatment. Especially in the latter, pre- and post-surgical evaluations of extracranial-intracranial arterial bypass surgery has been largely based on SPECT findings.[4,6,7] However, the procedure involves arterial blood sampling, ionizing radiation, and the use of vasodilatory agents, such as acetazolamide (ACZ) or carbon dioxide, that impose additional burdens on patients with a range of complications.[8,9] Efforts are still underway to replace these techniques with new alternatives that are less invasive and demanding.

Recently, temporal-shift (TS) analysis on resting-state functional MRI (rs-fMRI), which involves generating a TS map from low-frequency fluctuation of blood oxygen level-dependent (BOLD) signals, has been introduced to evaluate the hemodynamic state. These studies have shown that the local time shift of the BOLD signal is correlated with the prolongation of

perfusion parameters, such as the mean transit time (MTT) and time to peak (TTP), in patients with acute and chronic cerebral ischemia,[10-13] as well as in healthy subjects.[14] These lines of evidence suggest that the TS of BOLD primarily reflects vascular structure[14-16] and that the local TS of BOLD and perfusion parameters exhibit the same behavior in cerebral ischemia. Observable changes in venous drainage with increases in age further supports the technique and its underlying principles as experiential evidence. [16] Given that these perfusion parameters mirror CVR impairment in chronic ischemia, via compromised hemodynamics such as reduced velocity of a collateral pathway [17-20], some degree of agreement is expected between the TS map from rs-fMRI and SPECT-based CVR in these patients. Assessing CVR impairment using non-invasive BOLD MRI without vasodilatory stimuli, such as carbon dioxide (CO_2) or ACZ, would have a clinical impact on the management of patients with chronic ischemia. In the present study, we aimed to examine the capability of the method in evaluating the hemodynamic impairment of the patients with arterial occlusive diseases via comparison with CVR calculated by ACZ-challenged SPECT.

Materials and Methods

This is a cross-sectional evaluation of the equivalency between SPECT- and BOLD signal-based imaging methods in detecting hemodynamic impairment.

Participants

From April 2014 to July 2016, we prospectively recruited 28 patients with arterial occlusive diseases (21 with MMD and seven with atherosclerotic diseases) who were diagnosed on routine magnetic resonance angiography and successfully underwent ACZ-challenged

iodine-123 N-isopropyl-p-iodoamphetamine (^{123}I-IMP) SPECT scans for clinical purposes, at the university hospital. Patients with MMD were diagnosed according to a diagnostic criteria.[21] Patients with moderate to severe (>50%) stenosis/occlusion in the carotid or middle cerebral artery (MCA) were included in the atherosclerotic group. Since the hemodynamic change following acute stroke is a dynamic process,[22,23] we excluded patients who had a history of stroke events within a month before the SPECT scans. We also excluded three patients with MMD and two patients with atherosclerotic diseases who had large lesions extending over multiple MCA subdivisions [24] and/or the anterior or posterior cerebral artery (ACA or PCA) territories or a prominent focal symptom including hemiplegia and visual field defects that could moderate the global BOLD signal.[25,26] Finally 23 patients were enrolled in this study. (nine men and 14 women; mean age, 40.2 ± 17.9 years). Among 18 patients with MMD, nine patients had undergone revascularization surgery 2 months or more before the current study. Cortical infarctions (<5 mL) were found in four patients during routine MRI scans (Supplemental Digital Content 1, Figure 1). Cerebral angiography was performed according to the diagnostic criteria of MMD or for the evaluation of cerebral hemodynamics in patients who might have been candidates for surgical revascularization. The patient characteristics are summarized in **Table 1**.

This study was approved by our institutional review board/ethics committee (IRB C1002). The participants provided written informed consent in advance. To avoid the effect of ACZ on the TS map, rs-fMRI data were acquired before or one day following ACZ-challenged SPECT.

Imaging procedures

SPECT data acquisition and analysis

Dynamic SPECT data were acquired with a 2-head rotating gamma camera (Infinia, GE Medical Systems, Milwaukee, WI, USA) that featured an extended low-energy general-purpose collimator. For baseline SPECT, ^{123}I-IMP at 167 MBq was injected intravenously over 1 min when the data acquisition began. Arterial blood sampling was performed 10 min after data acquisition was initiated. For ACZ-challenged SPECT, ACZ (17 mg/kg) was injected 10 min before ^{123}I-IMP was injected and the data acquisition was started. The data were acquired over a 28-min period through a 360° rotation at a rate of 180°/min. Images were reconstructed and the cerebral blood flow (CBF) value was calculated with the QSPECT software package using the Transmission Dependent Convolution Subtraction method.[27,28] Each SPECT image was spatially normalized into 4-mm isotropic voxels using the SPECT template provided by SPM12 (Statistical parametric mapping, from the Wellcome Department of Cognitive Neurology, London, UK). CVR was calculated as follows: 100 × (ACZ scan - baseline scan)/baseline scan.

MR imaging data acquisition

A 3-T whole-body scanner (Tim-TRIO, Siemens, Erlangen, Germany) with a 32-channel phased-array head coil was used. BOLD rs-fMRI acquisition was performed using a multiband gradient-echo echo-planar imaging protocol from the University of Minnesota [29] with the following parameters: TR/TE = 1100/35 ms; flip angle = 60; matrix = 96 × 96 on a 192 × 192 mm^2 field of view; multiband factor = 6; and 72 2.0-mm-thick slices parallel to the anterior commissure-posterior commissure line. Only one run lasting 440 s (400 volumes, 7 min 20 s) was acquired, during which the patients were asked to stay still with their eyes open. A

three-dimensional structural image was also acquired (MP-RAGE, TR/TI/TE = 1900/900/2.58 ms; 256 × 256 × 192 voxels over a 230 × 230 × 170 mm sagittal slab).

MR imaging analysis

Preprocessing

The data were preprocessed using FSL (http://www.fmrib.ox.ac.uk/fsl) and SPM12 on MATLAB (MathWorks, Natick, MA, USA). The volumes corresponding to the first 10 s were discarded to ensure stationarity. Head motion was compensated for through two steps: regressing out the parameters obtained in the motion correction procedure and data scrubbing.[30] The scrubbing procedure involved searching the realigned time series for either (1) a global signal change of more than 0.5% between consecutive acquisitions or (2) abrupt head motion exceeding ± 3 mm or ± 3° per 0.5 s. Those contaminated time points were replaced with linearly interpolated values.[31] Finally, a temporal band-pass filter (0.02–0.12 Hz) was applied.[14,15,32]

To conduct a group analysis, nonlinear warping to the Montreal Neurological Institute template brain[33] was performed on the T1 anatomical images and functional volumes were normalized by using these parameters and were re-sliced to result in 4-mm isotropic voxels to assure adequate temporal signal-to-noise ratio in each voxel. Spatial smoothing was applied to the volumes by using an 8-mm full width at half maximum (FWHM) Gaussian kernel.

Creating BOLD temporal-shift map (TS map)

The method for creating the TS map is described in detail elsewhere.[15] We created the TS map with a recursive procedure which we predicted to be robust enough to effectively represent local blood circulation.[34] A schematic diagram of the procedure is shown in **Figure 1A**. To

create the initial reference time course, we used the global mean signal, which has commonly been used in previous studies [10-12]. Cross-correlations between this reference time course and every brain voxel were calculated to identify those with the highest correlation at a time shift of zero. By using this group of voxels, the global mean signal phase thus served as the reference time point (lag = 0 s) as the initial seed for the recursive procedure.

In each step of the recursive procedure, a cross-correlogram was calculated with the seed signal to obtain a set of voxels with a local peak at a time lag of ± 0.5 s. The reference time course was updated recursively at every step to the pooled signal from the voxels with the peak correlation at either 0.5 s or -0.5 s among three conditions: shifted by 0 s, ± 0.5 s, and ± 1 s. This procedure was repeated eight times for both the upstream and downstream directions to reach a ± 4 s tracking range. We thus created a TS map showing regions corresponding to -4 s, -3.5 s ...3.5 s, 4 s time shift relative to the global mean signal. The polarity of the TS was chosen so that the values represent phase advance and hence positive values indicate earlier arrival reflecting a "preferable" perfusion state. Peak correlation coefficients below 0.2 were ignored to prevent spurious correlations,[14] which allowed a considerable number of voxels to appear with no lag values. Such “holes” were filled by a Matlab script implementing a simple algorithm based on second-order partial differential equations (http://www.mathworks.com/matlabcentral/fileexchange/21214-inpainting-nan-elements-in-3-d). For voxel-wise analyses, in order to accomplish a smoothness comparable to that of the SPECT-based images, the resulting lag maps were further smoothed with an 8-mm FWHM box kernel.

Statistical analysis

To examine image similarity, a voxel-by-voxel Pearson's correlation coefficient (r) between the TS map and the SPECT-based images (CBF and CVR maps) was calculated for each patient. We used the vascular territory brain template, covering the whole-brain gray matter supplied by the anterior, middle, and posterior cerebral arteries (referred to as ACA, MCA, and PCA respectively) as a mask image to extract the values (**Fig. 1B**).[35] Using the z-transformed correlation coefficient [Z(r)] from each patient, image similarity with the TS map was evaluated with paired t-tests for CBF and CVR. To examine the association between the regional TS of BOLD signals and the SPECT-based CVR in each cerebrovascular territory, we performed region of interest (ROI)-based linear regression analyses, using the vascular territory brain template mentioned above (**Fig. 1B**). This template consists of three subregions (proximal, intermediate, and distal) in each vascular territory (ACA, MCA, and PCA). Among them, an intermediate template was chosen for the regression analyses so as to correctly represent each flow territory while minimizing the contribution from collateral circulation of other arterial trunks.[35,36] CVR in each ROI was compared using repeated-measures ANOVA followed by a post hoc Tukey test. Statistical analyses were conducted using the SAS Software *JMP Version 12.2* and MATLAB and P-values less than 0.05 were considered to be significant.

Results

Voxel-based image similarity between the TS map and SPECT images

The SPECT images and TS map from each patient are displayed in **Supplemental Digital Contents 2-5, Figures 2-5**. Images from a representative patient are shown in **Figure 2**. In the TS map here, voxel values indicate the phase advance of BOLD signal time-series relative to the

global signal, meaning that warm colors indicate earlier arrival.[15] The TS map clearly exhibited higher similarity to the CVR map than to the CBF map. This was confirmed by the voxel-by-voxel correlation analysis showing higher correlation with the CVR map in 21 out of 23 patients (**Fig. 3**). A group comparison using paired t-tests showed a significantly higher correlation between the TS map and the CVR map ([Z(*r*)] = 0.42 ± 0.18) than between the TS map and the CBF map ([Z(*r*)] = 0.058 ± 0.11) (*P* < .001). There were no significant disease group differences, but we found a negative correlation between the image similarity of TS with the CVR map Z(*r*) and the mean CVR in the bilateral MCA ROIs (r = -0.54, P = 0.0074), suggesting high accuracy of the technique in severe cases.

ROI-based regression analysis between the TS of BOLD signals and CVR

The ROI-based regression analyses revealed a significant linear effect of the TS of BOLD signals on CVR in the bilateral ACA and MCA ROIs, but not in the PCA ROIs (**Fig. 4A**). The group comparison using ANOVA revealed a significant decrease in CVR among these ROIs [F (2, 111.8) = 46.0, *P* < .001]. The post hoc test showed that CVR was highest in the PCA ROIs than in the two anterior flow territories (ACA and MCA ROIs) (**Fig. 4B**, *P* < .001 by Tukey's test). Thus, a significant effect of TS on CVR was found in the area where CVR was relatively impaired.

Discussion

Voxel-by-voxel analyses demonstrated relatively good agreement between the TS map from rs-fMRI and the CVR map calculated via ACZ-challenged SPECT when compared to the former's agreement with the CBF map at rest, although with considerable variation across

patients. While the interpretation of the TS of the BOLD signal time-series remains to be standardized, it theoretically tracks the propagation of a hemoglobin-related signal component that is thought to be intrinsic to blood.[14] Accordingly, studies have demonstrated an association of the TS map with perfusion delay parameters, such as MTT or TTP,[10-13] but not with CVR per se.[17-19] This is the first study to confirm the clinical significance of the BOLD TS analysis via comparison with a technique not based on temporal properties of the blood flow.

The ROI analyses further revealed a significant positive correlation between the TS value and the CVR, but only in the anterior circulation (the ACA and MCA territories) - not in the PCA territory where CVR was relatively preserved. In arterial occlusive diseases, a decrease in cerebral perfusion pressure induces protective mechanisms, such as compensatory vasodilation [1, 2] and collateral recruitment, both of which may affect the TS of BOLD signals.[11,12] Among these changes, compensatory vasodilation is detected by CVR in SPECT while perfusion delay affects the TS map. Despite the fundamental difference in target phenomena, a certain degree of severity of the ischemic condition can thus make a lesion concomitantly detected by the TS and CVR maps. This would account for the observed negative correlation between the CVR in the whole MCA territory and the image similarity between the TS and CVR maps; the more severe the impairment, the better the TS map resembles the CVR map. The low correlation observed in the PCA territory may also support this explanation.

The present study confirmed that the BOLD TS analysis has potential for the identification of the tissue at risk of ischemic stroke where CVR is impaired, without requiring radiation exposure or invasive procedures. CVR measured by BOLD (directly, without TS analysis) and arterial spin labeling has been proposed as a less invasive alternative to CVR measured by

ACZ-challenged SPECT.[37-40] Instead of ACZ, carbon dioxide (CO_2) is used as a vasodilator in this method. However, the manipulation of CO_2 requires patients to hold their breath or to inhale CO_2, which could cause transient complications such as headache and dizziness. Because of this, CVR measurement using CO_2 as a vasodilator occasionally fails to be completed in clinical practice.[41] In contrast, generating the TS map from rs-fMRI does not pose these issues as repeatedly emphasized in earlier works. Furthermore, this method is, at least computationally, equivalent to tracking the contrast agent injected instantaneously to the initial seed region, both anteriorly and posteriorly in time, but without the need for an exogenous contrast agent. Good reproducibility of TS analysis of BOLD signals has been addressed previously,[11] which is further enhanced by the recursive approach.[15] Altogether, the TS map would serve as a substitute for the CVR map calculated by ACZ-challenged SPECT and may also provide additional information about hemodynamics while producing far less patient burden in those with chronic cerebral ischemia.

One major caveat of this study may be the heterogeneity of the patient sample. We recruited consecutive patients who needed ACZ-challenged SPECT for the pre- or post-surgical evaluation of the hemodynamic state. As a result, 18 out of 23 patients had MMD including nine who had already undergone surgical revascularization. Effect of revascularization surgery is unclear because the sample size was insufficient for a subanalysis to draw any conclusion. Nevertheless, the heterogeneity does not necessarily indicate sampling bias because the study enrollees did represent the target population in need of SPECT-CVR. At the same time, our results showed a trend of higher similarity between the TS and CVR maps in patients with atherosclerotic diseases than in patients with MMD, suggesting a disease effect. Further studies

are thus warranted to examine the effect of the etiology of chronic cerebral ischemia on the TS map. A criteria or operative procedure for diagnosing CVR impairment should also be established. In a majority of the early studies, a simple approach was used where a certain delay relative to the global mean signal phase was treated as impairment.[10] However, setting a voxel-wise cutoff may not be straightforward because the phase varies across cortical regions. A data-driven approach such as supervised machine learning combined with a large healthy cohort may help to identify replacements for invasive techniques.

Future research should accommodate basic technical refinement of TS mapping. For example, an earlier report demonstrated the superiority of selecting the superior sagittal sinus (SSS) as an initial seed region for the TS analysis.[42] Indeed, this region has been frequently used in studies on lag mapping, including our own work.[14,15] Moreover, the disease itself modifies the global signal and special care is thus occasionally required when employing TS mapping, such as using only the unaffected hemisphere.[10,15] In the current study, two reasons account for our choice of the global signal over the SSS. First, we have found that SSS features an ageing-related phase shift relative to the global phase, which might confound the parametric analysis.[16] Second, we excluded those patients with large lesions or prominent focal symptoms to limit our analysis to normal brain tissue, for which previous research did not explicitly control. Hence, although BOLD TS map is considered to be robust against different seeds or tracking techniques,[15] SSS may constitute the optimal seed region for the general patient population. Another technical factor that may influence results of the TS analysis is the threshold of peak cross-correlation coefficient, which is used to suppress spurious correlation. While it seems reasonable to set a threshold, most earlier clinical studies did not take the spurious or negative cross-correlogram

peaks into account; hence, their assessments featured no holes to fill.[10,11,13] Tong and colleagues were the first to define a threshold; depending on the study, it was either 0.15 or 0.3. However, their research involved only healthy participants. [14,43] Standardization of the BOLD TS technique would thus require research with larger cohorts to establish empirically optimized parameters and reliable diagnostic criteria.

Conclusions

Although replication with a larger sample and technical refinement is warranted, the present results confirm that the BOLD TS analysis is a possible, non-invasive alternative to the current techniques for detecting hemodynamic impairment in arterial occlusive diseases.

References

1. Derdeyn CP, Videen TO, Yundt KD, et al. Variability of cerebral blood volume and oxygen extraction: stages of cerebral haemodynamic impairment revisited. *Brain.* 2002;125(Pt 3):595-607.

2. Powers WJ. Cerebral hemodynamics in ischemic cerebrovascular disease. *Annals of neurology.* 1991;29(3):231-240.

3. Gupta A, Chazen JL, Hartman M, et al. Cerebrovascular reserve and stroke risk in patients with carotid stenosis or occlusion: a systematic review and meta-analysis. *Stroke.* 2012;43(11):2884-2891.

4. Kuroda S, Houkin K. Moyamoya disease: current concepts and future perspectives. *The Lancet Neurology.* 2008;7(11):1056-1066.

5. Mandell DM, Han JS, Poublanc J, et al. Mapping cerebrovascular reactivity using blood oxygen level-dependent MRI in Patients with arterial steno-occlusive disease: comparison with arterial spin labeling MRI. *Stroke.* 2008;39(7):2021-2028.

6. Noh HJ, Kim SJ, Kim JS, et al. Long term outcome and predictors of ischemic stroke recurrence in adult moyamoya disease. *Journal of the neurological sciences.* 2015;359(1-2):381-388.

7. Pandey P, Steinberg GK. Neurosurgical advances in the treatment of moyamoya disease. *Stroke.* 2011;42(11):3304-3310.

8. Zimmermann S, Achenbach S, Wolf M, Janka R, Marwan M, Mahler V. Recurrent shock and pulmonary edema due to acetazolamide medication after cataract surgery. *Heart & lung : the journal of critical care.* 2014;43(2):124-126.

9. Hu CY, Lee BJ, Cheng HF, Wang CY. Acetazolamide-related life-threatening hypophosphatemia in a glaucoma patient. *Journal of glaucoma.* 2015;24(4):e31-33.

10. Lv Y, Margulies DS, Cameron Craddock R, et al. Identifying the perfusion deficit in acute stroke with resting-state functional magnetic resonance imaging. *Ann Neurol.* 2013;73(1):136-140.

11. Amemiya S, Kunimatsu A, Saito N, Ohtomo K. Cerebral hemodynamic impairment: assessment with resting-state functional MR imaging. *Radiology.* 2014;270(2):548-555.

12. Christen T, Jahanian H, Ni WW, Qiu D, Moseley ME, Zaharchuk G. Noncontrast mapping of arterial delay and functional connectivity using resting-state functional MRI: a study in Moyamoya patients. *J Magn Reson Imaging.* 2015;41(2):424-430.

13. Ni L, Li J, Li W, et al. The value of resting-state functional MRI in subacute ischemic stroke: comparison with dynamic susceptibility contrast-enhanced perfusion MRI. *Scientific reports.* 2017;7:41586.

14. Tong Y, Lindsey KP, Hocke LM, Vitaliano G, Mintzopoulos D, Frederick BD. Perfusion information extracted from resting state functional magnetic resonance imaging. *J Cereb Blood Flow Metab.* 2017;37(2):564-576.

15. Aso T, Jiang G, Urayama S-i, Fukuyama H. A Resilient, Non-neuronal Source of the Spatiotemporal Lag Structure Detected by BOLD Signal-Based Blood Flow Tracking. *Frontiers in Neuroscience.* 2017;11(256).

16. Satow T, Aso T, Nishida S, et al. Alteration of Venous Drainage Route in Idiopathic Normal Pressure Hydrocephalus and Normal Aging. *Frontiers in aging neuroscience.* 2017;9:387.

17. Kawano T, Ohmori Y, Kaku Y, et al. Prolonged Mean Transit Time Detected by Dynamic Susceptibility Contrast Magnetic Resonance Imaging Predicts Cerebrovascular Reserve Impairment in Patients with Moyamoya Disease. *Cerebrovasc Dis.* 2016;42(1-2):131-138.

18. Kikuchi K, Murase K, Miki H, et al. Quantitative evaluation of mean transit times obtained with dynamic susceptibility contrast-enhanced MR imaging and with (133)Xe SPECT in occlusive cerebrovascular disease. *AJR American journal of roentgenology.* 2002;179(1):229-235.

19. Kim JH, Lee SJ, Shin T, et al. Correlative assessment of hemodynamic parameters obtained with T2*-weighted perfusion MR imaging and SPECT in symptomatic carotid artery occlusion. *AJNR American journal of neuroradiology.* 2000;21(8):1450-1456.

20. Kluytmans M, van der Grond J, van Everdingen KJ, Klijn CJ, Kappelle LJ, Viergever MA. Cerebral hemodynamics in relation to patterns of collateral flow. *Stroke.* 1999;30(7):1432-1439.

21. Fujimura M, Tominaga T. Diagnosis of moyamoya disease: international standard and regional differences. *Neurol Med Chir (Tokyo).* 2015;55(3):189-193.

22. Huang YC, Tsai YH, Lee JD, et al. Hemodynamic factors may play a critical role in neurological deterioration occurring within 72 hrs after lacunar stroke. *PLoS One.* 2014;9(10):e108395.

23. Motta M, Ramadan A, Hillis AE, Gottesman RF, Leigh R. Diffusion-perfusion mismatch: an opportunity for improvement in cortical function. *Front Neurol.* 2014;5:280.

24. Barber PA, Demchuk AM, Zhang J, Buchan AM. Validity and reliability of a quantitative computed tomography score in predicting outcome of hyperacute stroke before thrombolytic therapy. ASPECTS Study Group. Alberta Stroke Programme Early CT Score. *Lancet.* 2000;355(9216):1670-1674.

25. Carter AR, Shulman GL, Corbetta M. Why use a connectivity-based approach to study stroke and recovery of function? *NeuroImage.* 2012;62(4):2271-2280.

26. Tsai YH, Yuan R, Huang YC, et al. Altered resting-state FMRI signals in acute stroke patients with ischemic penumbra. *PLoS One.* 2014;9(8):e105117.

27. Nishizawa S, Iida H, Tsuchida T, Ito H, Konishi J, Yonekura Y. Validation of the dual-table autoradiographic method to quantify two sequential rCBFs in a single SPET session with N-isopropyl-[123I] p-iodoamphetamine. *European journal of nuclear medicine and molecular imaging.* 2003;30(7):943-950.

28. Iida H, Narita Y, Kado H, et al. Effects of scatter and attenuation correction on quantitative assessment of regional cerebral blood flow with SPECT. *J Nucl Med.* 1998;39(1):181-189.

29. Feinberg DA, Moeller S, Smith SM, et al. Multiplexed echo planar imaging for sub-second whole brain FMRI and fast diffusion imaging. *PLoS One.* 2010;5(12):e15710.

30. Power JD, Barnes KA, Snyder AZ, Schlaggar BL, Petersen SE. Spurious but systematic correlations in functional connectivity MRI networks arise from subject motion. *NeuroImage.* 2012;59(3):2142-2154.

31. Mazaika PK, Hoeft F, Glover GH, Reiss AL. Methods and Software for fMRI Analysis of Clinical Subjects. *NeuroImage.* 2009;47:S58.

32. Tong Y, Frederick BD. Time lag dependent multimodal processing of concurrent fMRI and near-infrared spectroscopy (NIRS) data suggests a global circulatory origin for low-frequency oscillation signals in human brain. *NeuroImage.* 2010;53(2):553-564.

33. Evans AC, Collins DL, Mills SR, Brown ED, Kelly RL, Peters TM. 3D statistical neuroanatomical models from 305 MRI volumes. *Nuclear Science Symposium and Medical Imaging Conference, 1993, 1993 IEEE Conference Record.* 1993;3:1813-1817.

34. Tong Y, Frederick B. Tracking cerebral blood flow in BOLD fMRI using recursively generated regressors. *Human brain mapping.* 2014;35(11):5471-5485.

35. Mutsaerts HJ, van Dalen JW, Heijtel DF, et al. Cerebral Perfusion Measurements in Elderly with Hypertension Using Arterial Spin Labeling. *PLoS One.* 2015;10(8):e0133717.

36. Brozici M, van der Zwan A, Hillen B. Anatomy and functionality of leptomeningeal anastomoses: a review. *Stroke.* 2003;34(11):2750-2762.

37. Leoni RF, Mazzetto-Betti KC, Silva AC, et al. Assessing Cerebrovascular Reactivity in Carotid Steno-Occlusive Disease Using MRI BOLD and ASL Techniques. *Radiology research and practice.* 2012;2012:268483.

38. Pillai JJ, Mikulis DJ. Cerebrovascular reactivity mapping: an evolving standard for clinical functional imaging. *AJNR American journal of neuroradiology.* 2015;36(1):7-13.

39. Uchihashi Y, Hosoda K, Zimine I, et al. Clinical application of arterial spin-labeling MR imaging in patients with carotid stenosis: quantitative comparative study with single-photon emission CT. *AJNR American journal of neuroradiology.* 2011;32(8):1545-1551.

40. Yun TJ, Paeng JC, Sohn CH, et al. Monitoring Cerebrovascular Reactivity through the Use of Arterial Spin Labeling in Patients with Moyamoya Disease. *Radiology.* 2016;278(1):205-213.

41. Spano VR, Mandell DM, Poublanc J, et al. CO2 blood oxygen level-dependent MR mapping of cerebrovascular reserve in a clinical population: safety, tolerability, and technical feasibility. *Radiology.* 2013;266(2):592-598.

42. Wu J, Dehkharghani S, Nahab F, Allen J, Qiu D. The Effects of Acetazolamide on the Evaluation of Cerebral Hemodynamics and Functional Connectivity Using Blood Oxygen Level-Dependent MR Imaging in Patients with Chronic Steno-Occlusive Disease of the Anterior Circulation. *AJNR Am J Neuroradiol.* 2017;38(1):139-145.

43. Tong Y, Hocke LM, Fan X, Janes AC, Frederick Bd. Can apparent resting state connectivity arise from systemic fluctuations? *Frontiers in Human Neuroscience.* 2015;9:285-285.

Figure Legends

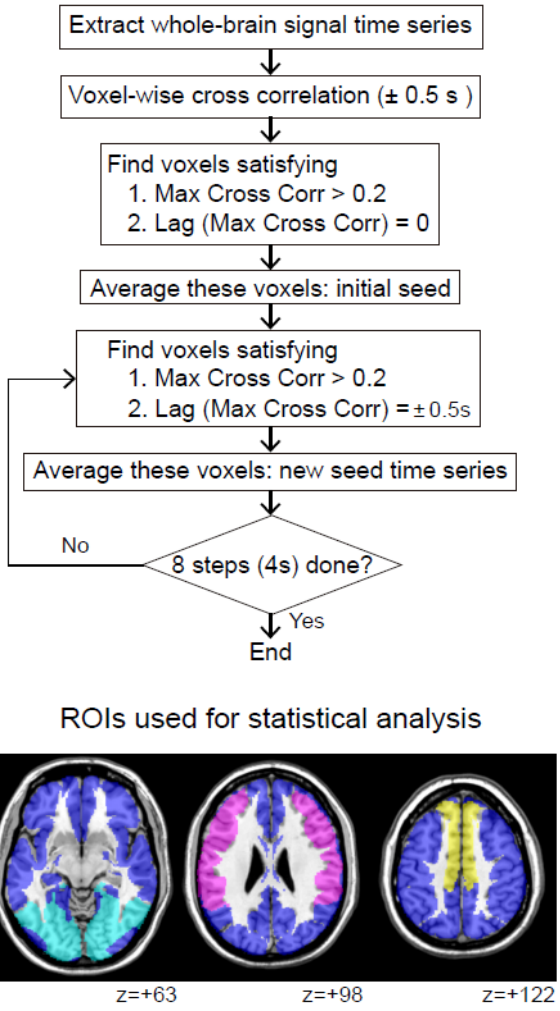

Figure 1. A schematic of the temporal-shift (TS) analysis and regions of interest (ROIs) used in the present study.

(A) A schematic of the analysis workflow.

(B) ROIs used for the voxel-wise correlation and regression analyses. All gray matter voxels were colored to indicate the mask used for the voxel-by-voxel correlation analyses (dark purple and the following three colors). ROIs for the anterior (yellow), middle (violet), and posterior (cyan) cerebral artery intermediate flow territories were used for the regression analyses.

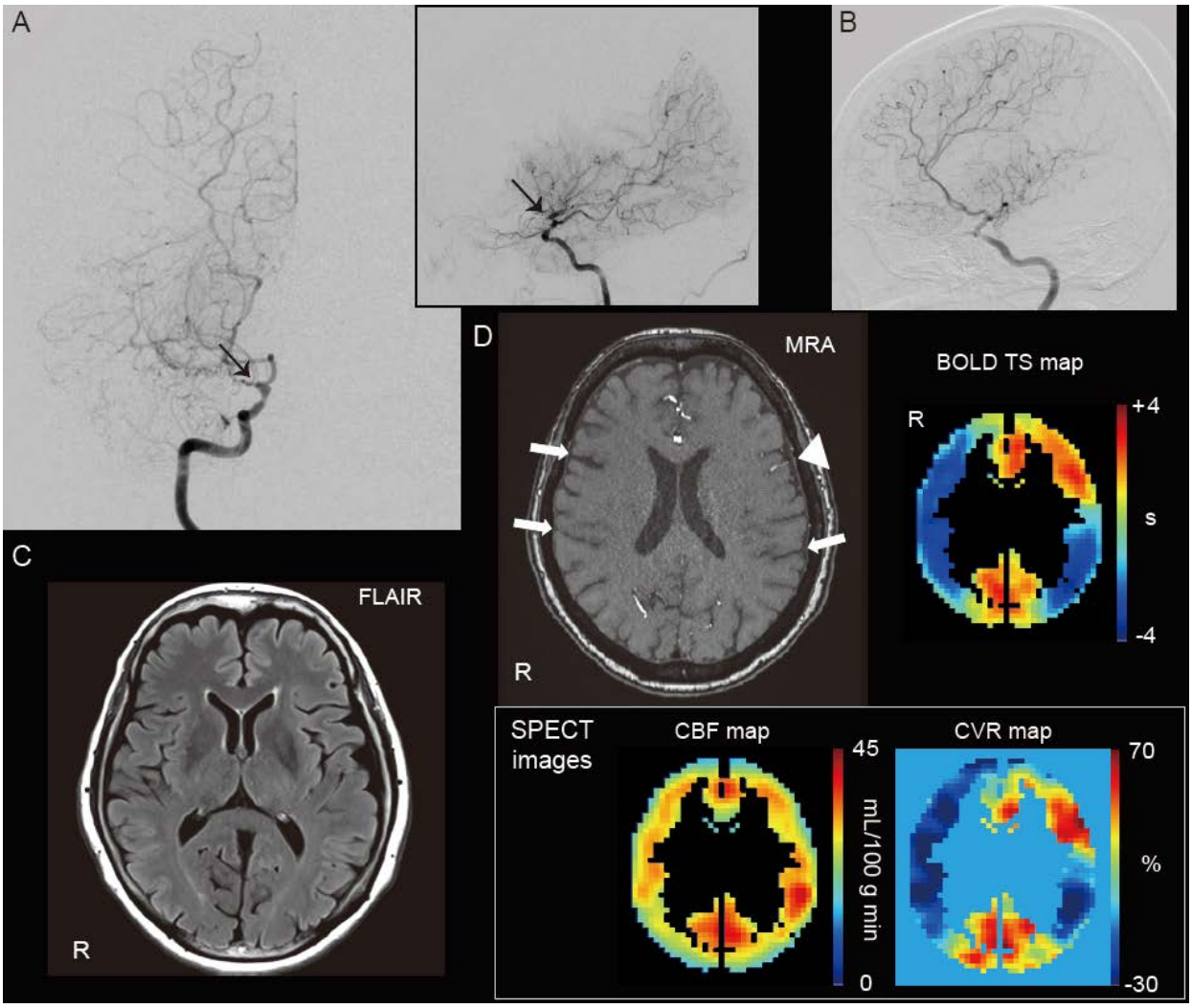

Figure 2. The TS map and single-photon emission computed tomography (SPECT) images in a representative patient (Patient No. 22, female, 65 years old) with bilateral atherosclerotic lesions.

(A) Right internal carotid artery (ICA) angiogram shows occlusion of the right ICA (arrows).

(B) Left ICA angiogram (right anterior oblique view) shows no filling of distal left MCA branches or collateral flow via leptomeningeal anastomosis in the distal left MCA.

(C) The fluid attenuation inversion recovery (FLAIR) image shows no abnormalities in the territory of bilateral MCAs.

(D) In the 3D time-of-flight magnetic resonance angiography axial source image (top left), the signal of the branches of the right and left MCA is not observed (white arrows), whereas the branch of the left MCA is preserved (white arrowhead). The cerebral blood flow (CBF) map measured by the baseline SPECT image (bottom left) shows no marked reduction in CBF in the MCA territories. In contrast, cerebrovascular reactivity (CVR) is decreased in the territories of the occluded MCAs (bottom right). The TS (top right) and CVR maps presented similar spatial pattern (top right). The positive values in the TS map indicate phase advances relative to the global signal phase, reflecting an early arrival of the blood.

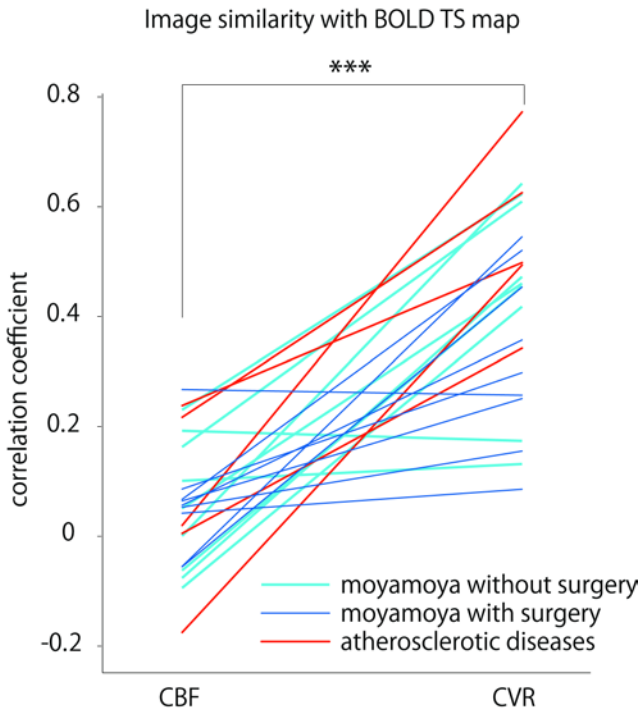

Figure 3. Voxel-by-voxel correlation of the TS maps with SPECT images in each patient.

The light blue/blue lines indicate patients with moyamoya disease; those who underwent revascularization surgery are shown in blue. The red lines indicate patients with atherosclerotic disease. TS maps from blood-oxygen-level-dependent (BOLD) signals are more closely correlated with CVR maps ([Z(*r*)] = 0.42 ± 0.18) than CBF maps ([Z(*r*)] = 0.058 ± 0.11).

*** = P < .001, paired-t test

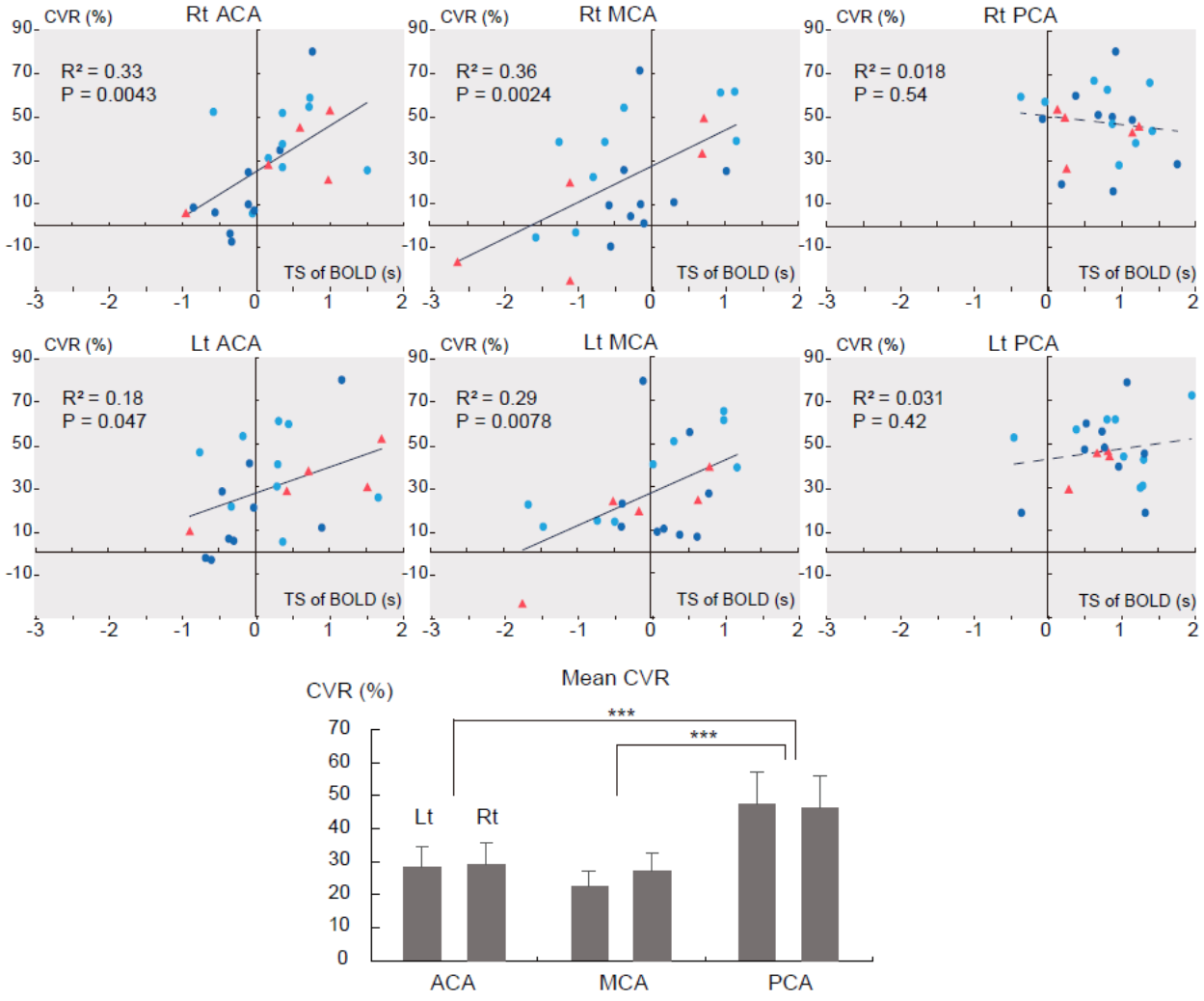

Figure 4. ROI-based regression analyses between the TS of BOLD signals and CVR in each cerebrovascular territory.

(A) A significant linear correlation between the BOLD TS value and CVR was observed in the anterior and middle cerebral artery ROIs. The light blue and blue circle plots indicate patients without and with surgery, respectively. The red triangle plots indicate patients with atherosclerotic diseases.

(B) Comparison of mean CVRs across the three vascular territories.

ACA = anterior cerebral artery, MCA = middle cerebral artery, PCA = posterior cerebral artery.

*** = P < .001, paired-t test on the combined values of both sides

Supplemental Digital Content 1. Figure 1. MR images showing the lesions of the four patients included in the study, with previous small infarcts.

Supplemental Digital Content 2. Figures 2. CBF, CVR and temporal shift (TS) maps from the patients 1-6.

Supplemental Digital Content 3. Figure 3. CBF, CVR and temporal shift (TS) maps from the patients 7-12.

Supplemental Digital Content 4. Figure 4. CBF, CVR and temporal shift (TS) maps from the patients 13-18.

Supplemental Digital Content 5. Figure 5. CBF, CVR and temporal shift (TS) maps from the patients 19-23.